Robust detection and segmentation of cell nuclei in biomedical images based on a computational topology framework

Wei Xiong

Ruprecht-Karls-Universität Heidelberg

xiong@thphys.uni-heidelberg.de

September 21, 2023

Overview

Segmentation in histological images is challenging

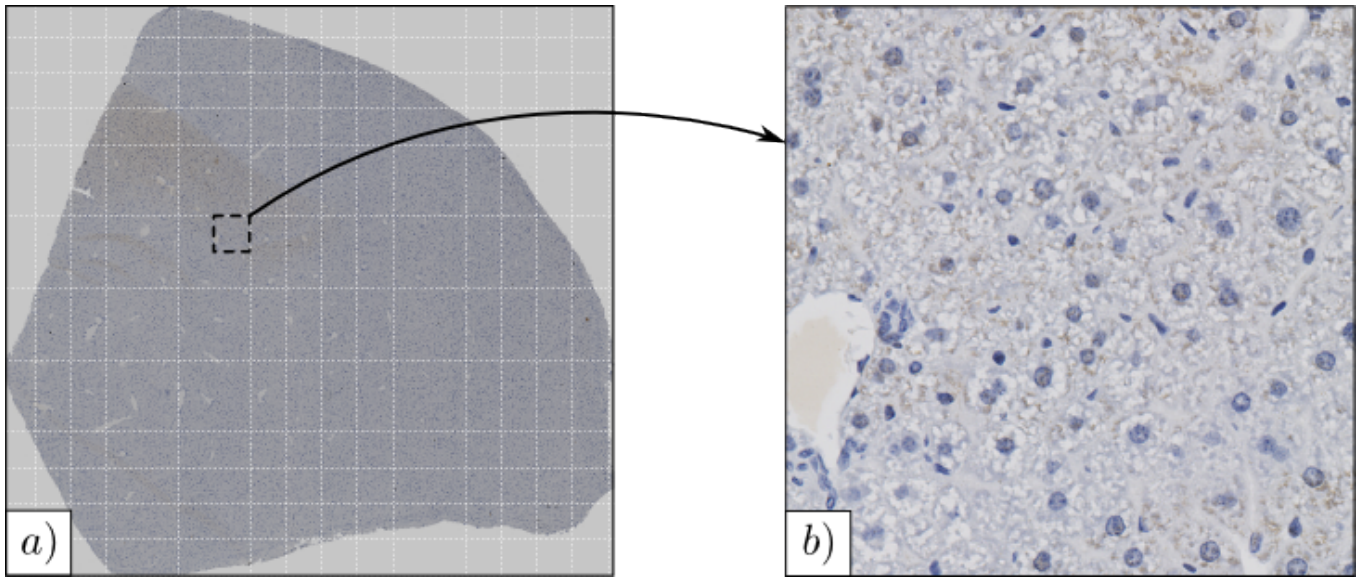

Figure: Sample liver section used in the analysis: a) whole slide image, and b) cropped square section. Glass slides are automatically imaged at high resolution in bright-field mode at a 40-fold magnification (0.23 µm/pixel) using the Hamamatsu NanoZoomer 2.0-HT (Hamamatsu Photonics, Japan) at TIGA Center Heidelberg.

Segmentation in histological images is challenging

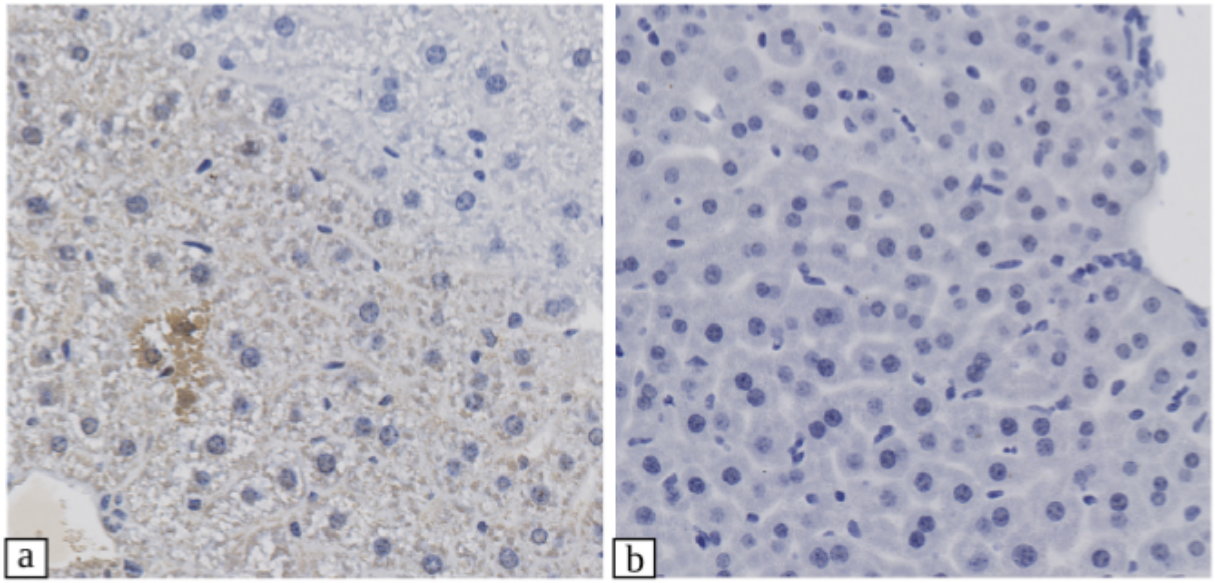

Figure: Example of histopathology images. a),b) 616^2 pixel Cropped images of liver injury induced by lipopolysaccharide, 40X, stained by Tyr705 D3A7 rabbit-HRP conjugated antibodies.

1

[1] Katja Breitkopf-Heinlein, Department of Medicine II, Faculty of Medicine at Mannheim, Heidelberg University, Mannheim, Germany.

Introduction

Image Features:

- Noise, clutter
- Low contrast
- Object complexity
- Occlusion
- Significant variance in appearance properties, shape, size, color, texture and distribution of regions of interest (ROIs) in histological sections.

Existing algorithm:

- Variational approaches to image segmentation
- The segmentation is presented in a probabilistic fashion, e.g. Probabilistic Graphical Models (PGMs).
- Machine learning methods, e.g. Support Vector Machines (SVM), Artificial Neural Networks (ANN), Convolutional Networks (CNN).
- Hybrid Approaches.

Method Pipeline

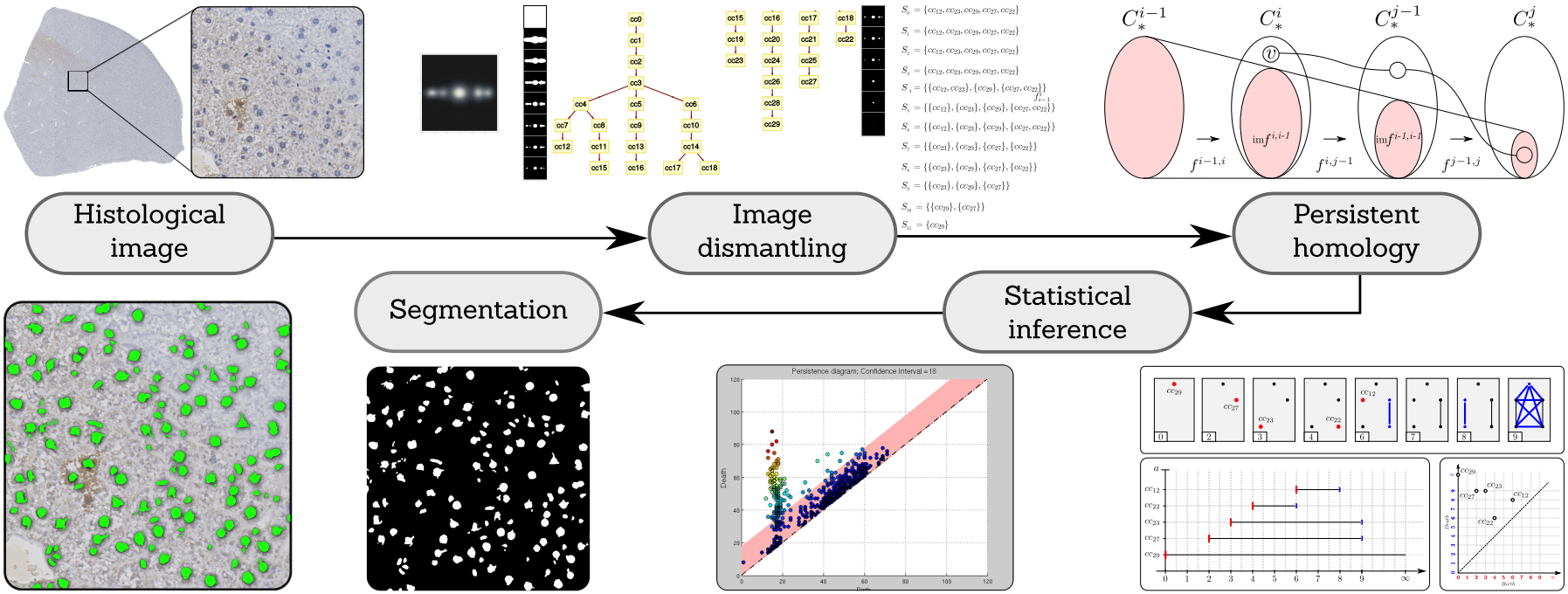

Figure: The Segmentation Method Pipeline

Image Dismantling and Inclusion Tree

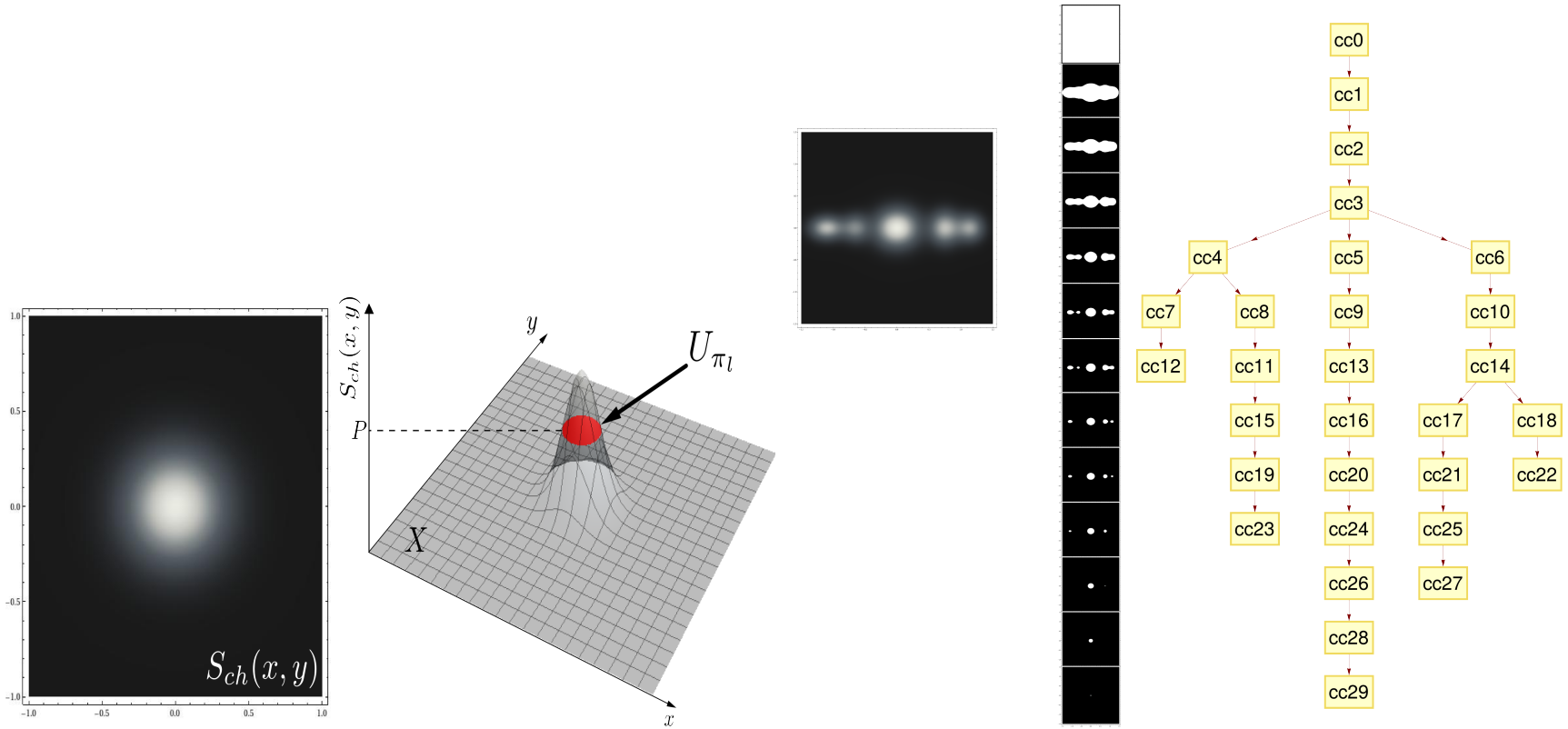

Figure: Image dismantling. Images are dismantled into connected components at different scales. An inclusion tree is built that stores parenthood information between connected components.

Image Dismantling

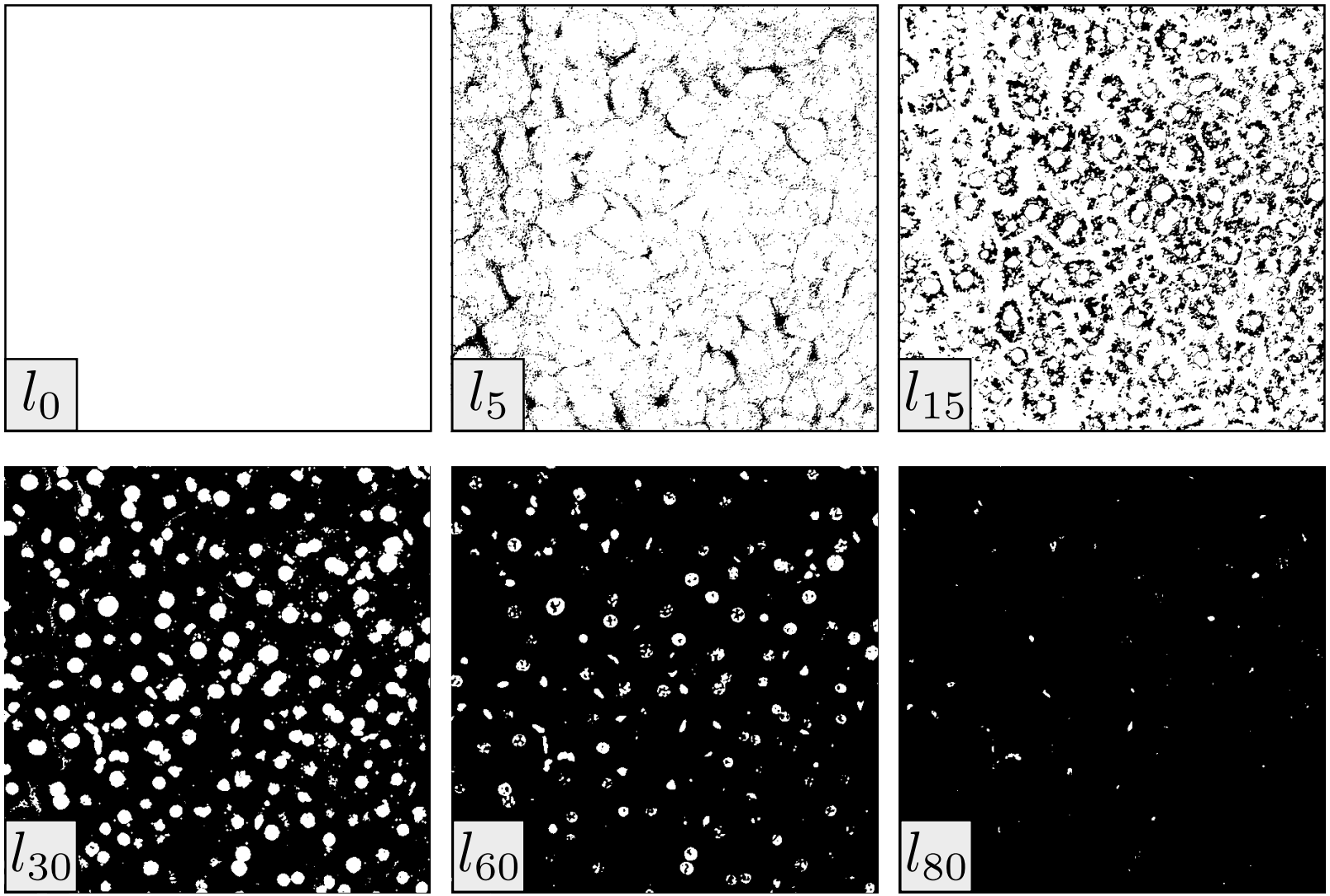

Figure: Example of projections obtained for a sample cropped image at dif- ferent level lines: l_0 , l_5 , l_{15} , l_{30} , l_{60} , and l_{80} .

Persistent homology

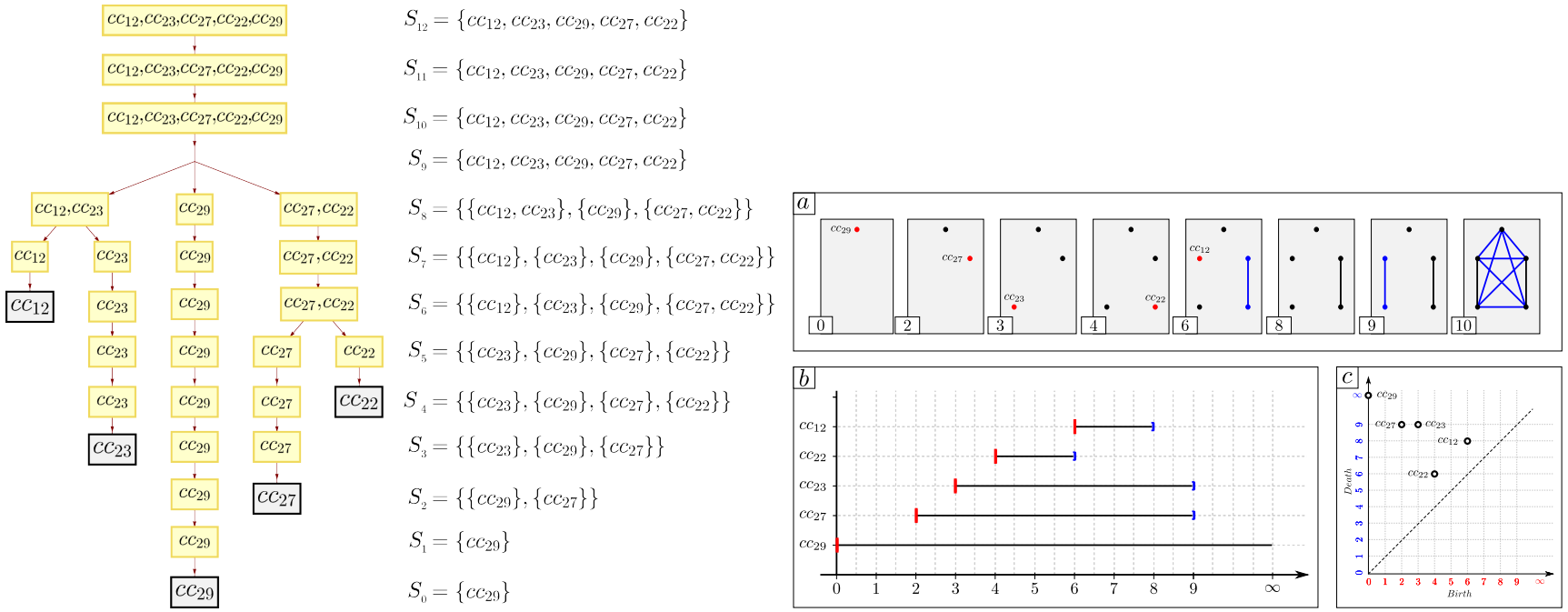

Figure: By traveling the inclusion tree from the leaves to its root a sequence of abstract simplicial complexes is spanned. Persistent homology is used to summarize homology changes when step.Process summary: a) Geometric representation of abstract simplicial complex at different level lines, b) persistent barcode visualization and c) persistent diagram showing the birth and death of topological features as points in the diagram.

LPS Hepatocytes

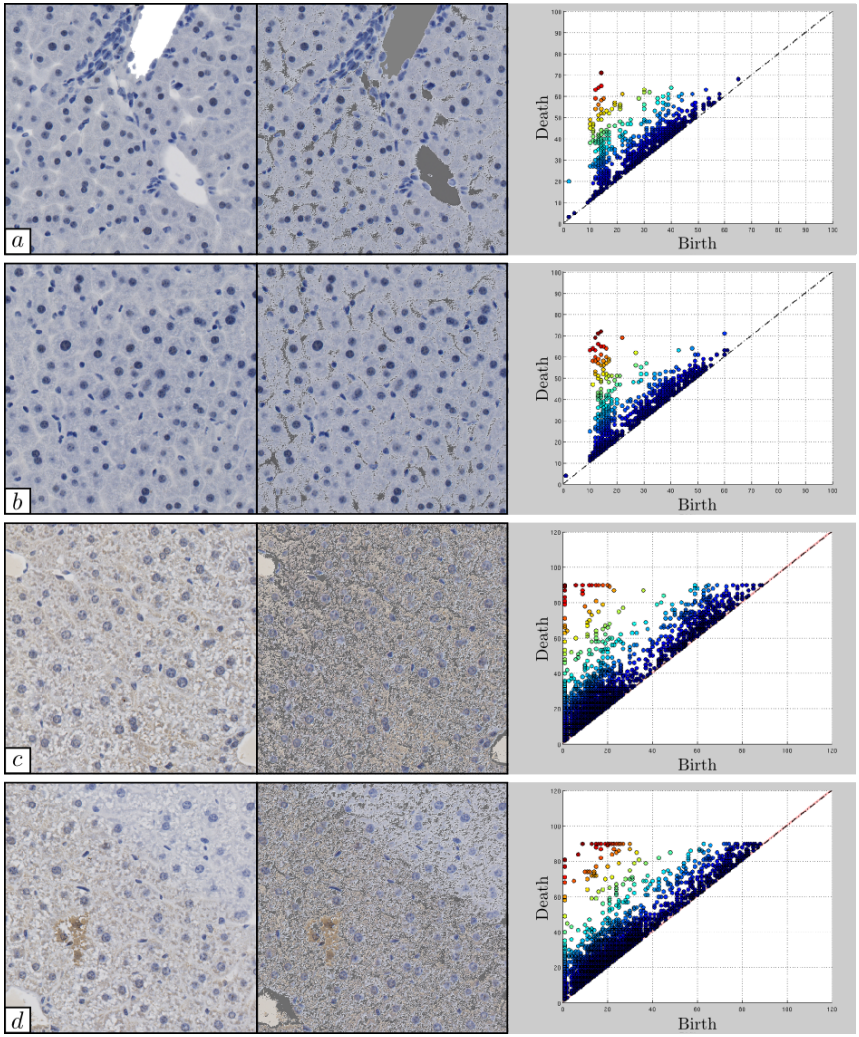

Figure: Four cropped histological sections (left) and their corresponding persistent diagrams for the homology group 0 (right) are shown. For each image a nontrivial segmented region is shown (middle); this is the segmented region that persists for two or more filtration steps.

LPS Hepatocytes

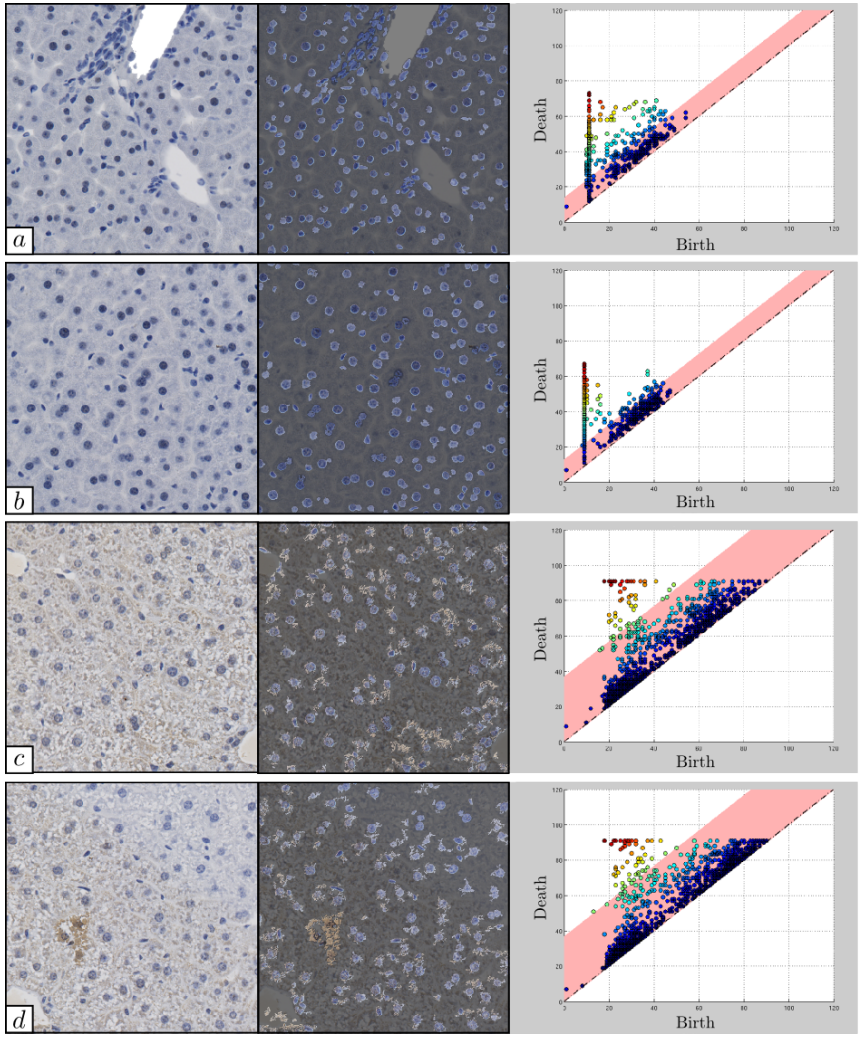

Figure: Using the histological sections of Fig. 28 (left) to obtain segmentations (middle) with an 80% confidence interval for the noise. The bands in the persistent diagrams (right) define regions where any point inside them is labeled as noise.

Results

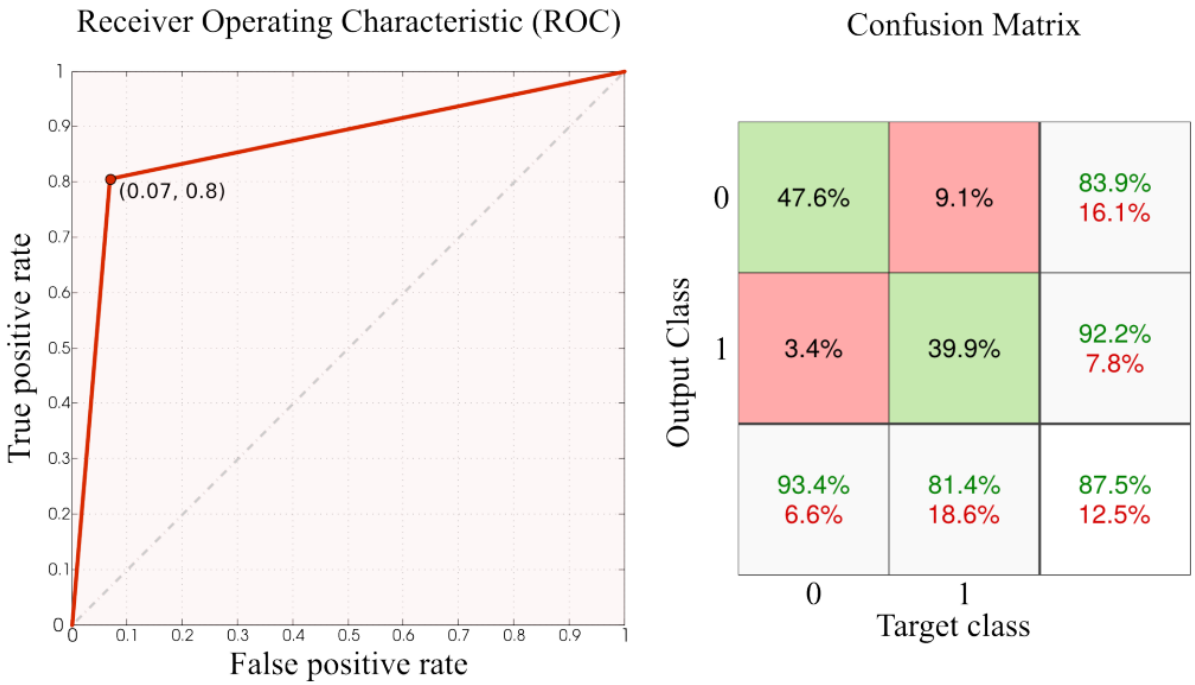

Figure: Average segmentation performance for all nuclei (hepatocyte and non-parenchymal cells). Normalization balances background (0) and nuclei class (1); each class contained approx. 50% of the data. Overall accuracy: 87.5%; error rate: 12.5%; specificity: 93.4%; true positive rate for nuclei: 81.4%; false positive rate: 6.6%.

Results

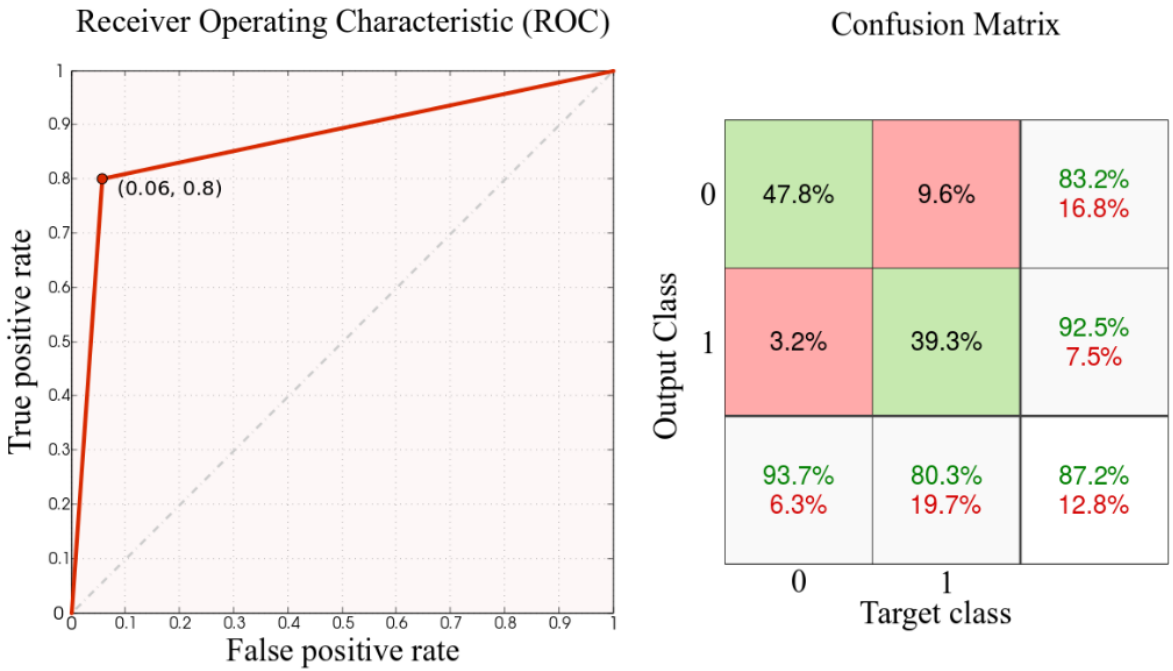

Figure: Average segmentation performance for hepatocyte cell nuclei. Normalization balances background (0) and nuclei class (1); each class contained approx. 50% of the data. Overall accuracy: 87.2%; error rate: 12.8%; specificity: 93.7%; true positive rate for nuclei: 80.3%; false positive rate: 6.3%.

Results

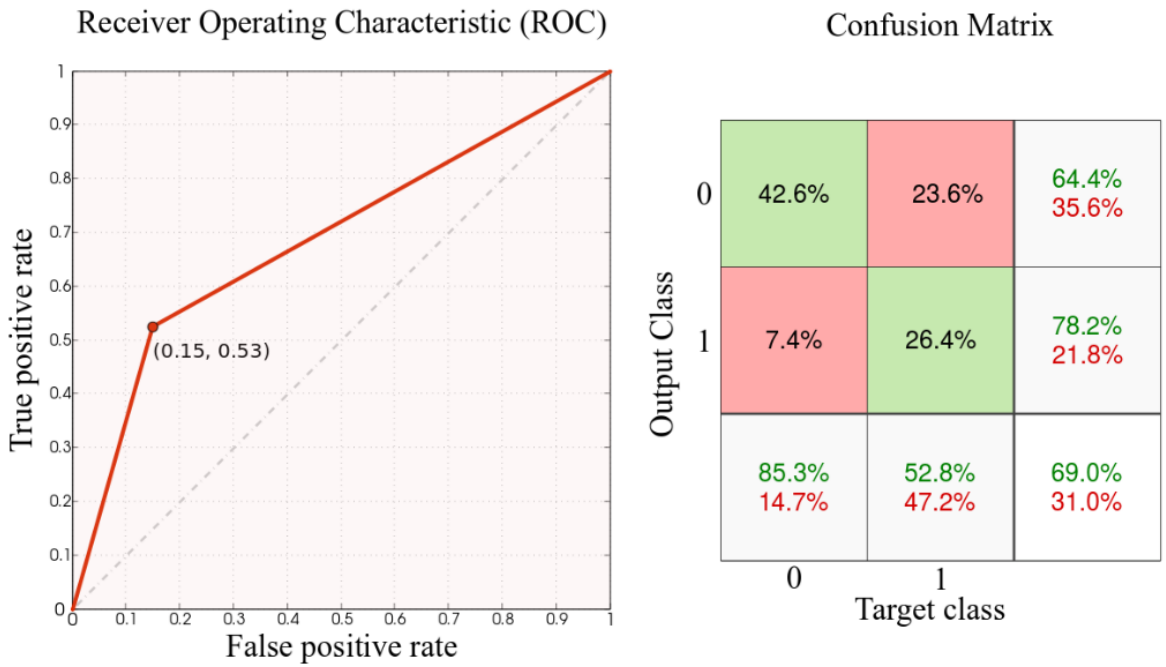

Figure: Average segmentation performance obtained with ilastik 1.1.8 for all nuclei (hepatocyte and non-parenchymal cells). Ilastik is trained with the same two images used for tuning the proposed approach. Normalization balances background (0) and nuclei class (1); each class contained approx. 50% of the data. Overall accuracy: 69.0%; error rate: 31.0nuclei: 52.8%; false positive rate: 14.7%.

Related Publication and Aknowledges

R. Moraleda, Wei Xiong, B. Lenoir, N. Valous, Niels Halama (2021)

Detection and segmentation of capillary structures in biomedical images based on a computational topology framework

AMS: Advances in Computational Biomedicine
https://meetings.ams.org/math/jmm2021/meetingapp.cgi/Paper/3030.

R. Moraleda, W. Xiong, B. Lenoir, N. Valous, N. Halama (2020)

Segmentation of biomedical images based on a computational topology framework

Seminars in Immunology Vol 48, Academic Press, DOI:Seminars in immunology 10.1016/j.smim.2020.101432.

R. Moraleda, W. Xiong, B. Lenoir, N. Valous, N. Halama (2019)

Computational Topology for Biomedical Image and Data Analysis: Theory and Applications

CRC Press Focus Series in Medical Physics and Biomedical Engineering, ISBN: 9780429443077, DOI: 10.1201/9780429443077.

R. Moraleda, W. Xiong, B. Lenoir, N. Valous, N. Halama (2017)

Robust detection and segmentation of cell nuclei in biomedical images based on a computational topology framework

*Medical image analysis*Vol 38, pages 90-103, DOI: 10.1016/j.media.2017.02.009.

Thanks!